Coupling the actuator line method to the high order meteorological LES model Meso-NH to study wind farm wakes impacts on local meteorology

IOP Conf. Series: Journal of Physics: Conf. Series **1256** (2019) 012019 doi:10.1088/1742-6596/1256/1/012019

Coupling the actuator line method to the high order meteorological LES model Meso-NH to study wind farm wakes impacts on local meteorology

PA Joulin[1,2], ML Mayol[3,4], F Blondel[2], V Masson[1], Q Rodier[1] and C Lac[1]

[1] Meteo France, CNRM, 42 Avenue Gaspard Coriolis, 31057 Toulouse, France
[2] IFP Energies Nouvelles, 1-4 Avenue du Bois Prau, 92852 Rueil-Malmaison, France
[3] FCEyN, University of Buenos Aires, Av. Intendente Giraldes 2160 - Ciudad Universitaria, C1428EGA, Buenos Aires, Argentina
[4] Computational Simulation Center, CSC - CONICET, Godoy Cruz 2390, C1425FQD, Buenos Aires, Argentina

E-mail: pierre-antoine.joulin@meteo.fr, mlmayol@csc.conicet.gov.ar

Abstract. Offshore wind energy is now reaching the technological maturity, its capacity is increasing all over the world and this trend is projected to continue for several more years. Given this expectation, a better understanding of the relationship between the presence of wind farms and the atmospheric boundary layer is needed. Turbulent wakes produced by wind turbines can significantly impact the flow dynamics within wind farms and downstream of them. Operating offshore parks have already shown losses on energy production and effects on the local climate. In order to analyse the interactions occurring during these impacts, a new tool has been developed. This numerical tool is a coupling between the Actuator Line Method (ALM) and the open-source, non-hydrostatic mesoscale atmospheric model Meso-NH, based on the Large Eddy Simulation (LES) framework. The coupled Meso-NH + ALM system is first validated by using the experimental data obtained during the New MEXICO experiments. In particular, simulated and experimental loadings along the blades are compared. Then, a simulation of an idealized Horns Rev wind farm is performed using met mast measurements and reanalysis data for the "Horns Rev 1 photo case" as initial conditions. This new coupled system allows the exploration of the impact of wind farms on the lower levels of the atmosphere.

1. Introduction

In the path of the decarbonization of the electricity sector, offshore wind energy is becoming one of the main actors. This technology has reached its maturity and therefore it is much more competitive now. Taking into account where the wind turbine market is heading, under the paradigm "Bigger is better", offshore turbines today are growing in size very fast. While the swept area of the turbines becomes larger, their interaction with the lower layers of the atmosphere deepens. In fact, turbulent wakes produced by wind turbines can significantly impact the flow dynamics within wind farms and downstream of them. Operating offshore parks have already shown losses on energy production [1] and effects on the local climate [2].

To analyze these interactions, an accurate representation of processes occurring between the atmospheric boundary layer, the surface and the wind turbines is necessary. It can be done

with a wide variety of numerical tools, among which the Computational Fluid Dynamics (CFD) models are found. Several approaches can be considered to compute the Navier-Stokes equations, such as the Reynolds Averaged Navier Stokes (RANS), the Large Eddy Simulation (LES) or the Direct Numerical Simulation (DNS). Nevertheless, RANS is not a proper method to analyze the instantaneous wake of a wind turbine because it only solves mean flow while modelize turbulence aspects. On the other hand, the DNS method is more accurate but numerically too expensive because it computes all turbulent scales. In this study, the meteorological model Meso-NH is used in its LES framework to simulate the atmospheric boundary layer. The LES method consists in resolving the large scales and modelizing the smaller ones, while wind turbines are represented by Actuator Lines Method (ALM). Besides, Meso-NH takes into account atmospheric phenomena such as buoyancy, humidity and precipitations.

This coupled model will be first validated through comparisons with experimental data from measurements performed in a wind tunnel. Even if the tool has been designed to analyze wind farms at a real scale, accurate data are too rare at this scale to do a comparison. This is why the New MEXICO experiments [3] have been chosen to evaluate the new solver. Then, Meso-NH will be used to simulate the Horns Rev 1 Photo Case [2], showing a wake fog generated by the wind farm on the morning of February 12, 2008. To reproduce this phenomenon, a reduced wind farm will be placed into an idealized meteorological environment based on met-mast measurements and reanalysis data obtained for that day.

2. Numerical Method

2.1. Meso-NH

Developped by the Centre National de Recherche Météorologique (CNRM - CNRS/Météo France) and the Laboratoire d'Aérologie (LA - UPS/CNRS), Meso-NH is an open-source CFD model which can simulate atmospherical flows from meso to micro-scales [4]. Meso-NH is based on a non-hydrostatic equation system. The dynamical part is described in [5] and can be computed using a LES framework,. A 1.5 order closure system is used to evaluate the 3 dimensional turbulence ([6], [7], [8], [9]). A prognostic equation is used for the subgrid kinetic energy and the mixing length is parameterized. Among the mixing length parametrization available, the one of Deardorff [10] was chosen for this study.

A pressure solver diagnoses the pressure field through an elliptic equation solved by an iterative method. This equation is obtained by merging continuity and momentum equations. Besides, Meso-NH is an anelastic model based on the pseudo-compressible system of Durran [11], that filters elastic effects from sound waves. The approach is Eulerian and the discretization is performed using an Arakawa C-grid [12]. Wind advection (*i.e.* transport) is treated using a 4th order centered spatial scheme combined with the explicit Runge Kutta centered 4th order scheme for time integration. Computations are horizontally parallelized [13] and the vertical coordinate can be non-regular thanks to a stretching, giving the opportunity to increase the resolution in the region of interest.

2.2. Actuator Line Method

Introduced by Sørensen and Shen [14], the Actuator Line Method allows to represent the three blades and their motion using a body force approach. This technique, compared to the actuator disc model ([15], [16]), gives a better description of the wake behind the wind turbines. In fact, it can reproduce the helical shape of the wake and also generate the root and tip vortices ([17], [18], [19], and [20]). This method has been coupled with different LES solvers ([21], [22] [23], [24]) to simulate wind turbine and wind farm flows.

The ALM consists in representing the blades by lines carrying body forces over several blade element points, applying efforts against the flow. These aerodynamic forces $\overrightarrow{dF}$ are determined

thanks to a blade element approach:

$$\overrightarrow{dF} = \frac{1}{2}\rho c \left\|\overrightarrow{U_{rel}}\right\|^2 (C_L\overrightarrow{e_L} + C_D\overrightarrow{e_D})dr, \quad (1)$$

where c and dr are respectively the chord and the length of the blade element and ρ the air density. $\overrightarrow{U_{rel}}$ is the relative velocity composed by the wind speed $\overrightarrow{U_{wind}}$ and $\overrightarrow{U_\Omega}$, the opposite of the tangential blade element speed, as shown in Figure 2. Both the lift and drag coefficients (C_L and C_D) depend on the airfoils characteristics, and are evaluated through a cubic spline interpolation of tabulated data. As shown in Figure 2, $\overrightarrow{dF}$ is a combination of the drag force $\overrightarrow{dF_D}$ acting in the direction of $\overrightarrow{U_{rel}}$ (along the unit vector $\overrightarrow{e_D}$), and the lift force $\overrightarrow{dF_L}$, perpendicular to the last one (along the unit vector $\overrightarrow{e_L}$).

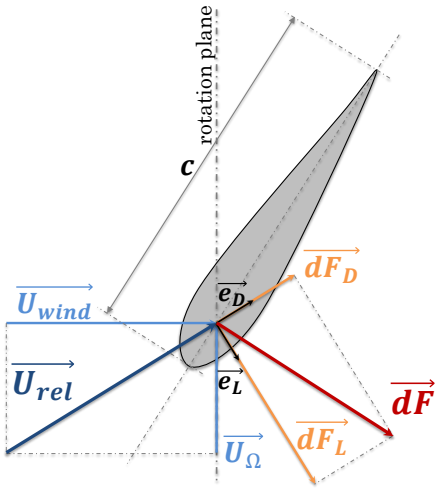

Figure 1. 2D blade element velocities and forces

2.3. Coupled system

Meso-NH and the Actuator Line Method are both exchanging information. The position, orientation matrix and the velocity of blade element points are computed at each time step. Knowing these positions, the ALM can exploit fluid properties (such as ρ and U_{wind}) from the 3D fields of Meso-NH at the last time step in order to calculate the aerodynamic force $\overrightarrow{dF}$ (Eq. 1). The wind velocity U_{wind} is obtained using a tri-linear interpolation of the eight neighboring cells of Meso-NH, surrounding the blade element point. Then, the norm of the aerodynamic force is added to the momentum equation of Meso-NH:

$$m\frac{\partial\overrightarrow{U_{wind}}}{\partial t} = \overrightarrow{Adv} + \overrightarrow{Cor} + \overrightarrow{Pres} + \overrightarrow{Turb(U_{wind})} - \overrightarrow{dF}, \quad (2)$$

where $\overrightarrow{Adv}$ is the advection term, $\overrightarrow{Cor}$ the Coriolis term, $\overrightarrow{Pres}$ the pressure gradient term, and $\overrightarrow{Turb}$ the turbulence term. A regularization kernel is commonly used in order to avoid numerical singularities ([14], [17]). Further studies also give guidelines about optimal volume force distribution regarding the kernel shape ([25], [26], [27]). Nevertheless, the forces are distributed smoothly over several flux points by calculating the average effort of the two nearby mass points. It shows similar results, avoiding instabilities and the calculation cost of the convolution product. Besides, even if the tip loss correction of Glauert [28] should not be used for the ALM, it has been used to alleviate the over-predicted loads at the blade tip region, as proposed by [17]. To avoid this correction, an improved load distribution will be developed in future work as advised in [29].

3. Validation

3.1. The New MEXICO experiments

The New MEXICO (Model Experiment in Controlled Conditions) experiments [3] have been carried out in the German Dutch Wind Tunnel, using the Large Scale Low Speed Facility and its 9.5 m x 9.5 m open section. The wind turbine is a 4.5 m diameter, three blades rotor. The twisted and tapered blades are based on DU91-W2-250, RISØ-A1-21 and NACA64-418 airfoils from root to tip. Three different flow cases have been simulated: 10m/s, 15m/s and 24m/s. For each case, the rotational velocity of the wind turbine Ω and the pitch angle of the blade β are constant (Ω = 424.5rpm ; β = -2.3°). No initial turbulence is considered. The integration of pressure taps allows to obtain the normal and tangential loads at five positions.

3.2. Numerical Set-Up

The three cases have different air conditions, described in Table 1. As inputs, the wind speed u, the potential temperature θ and the pressure p have been used, giving a density ρ at hub height which corresponds to the experimental one. The wind velocity profile is constant and the thermal conditions are neutral.

Table 1. Air condition description of the three studied cases simulated by Meso-NH

Cases	n°1	n°2	n°3
$u(m/s)$	10.05	15.06	24.05
$\theta(K)$	293.65	295.0	294.15
$p(Pa)$	101398	101345	101407
$\rho(kg/m^3)$	1.197	1.191	1.195

The domain size is about $L_x = 40m \times L_y = 30m \times L_z = 30m$ and the center of the rotor is placed at coordinates $(15m, 15m, 15m)$. A $\Delta x = \Delta y = \Delta z = 0.1m$ resolution has been chosen for the LES simulations, and 42 elements per blade have been used for the ALM. The lateral and upper borders are opened. The upstream border generate a constant wind given in Table 1. Because Meso-NH can not simulate a domain without a surface friction on the ground, wind turbine is placed at a high level in order to neglect the effect of the small boundary layer developed. The nacelle and the tower are not represented. As explained in Section 2.3, the average method for the force distribution and the tip loss correction are activated. The time step, about $\Delta t = 0.001sec$, is chosen such that the blade tip does not traverse more than one grid cell during a time step.

3.3. Results

The results of the simulations are compared to the experimental data from New MEXICO experiments, focusing on the normal forces along the blade span in Figure 2. They are also confronted to CASTOR and SOWFA. CASTOR is a free wake vortex filament lifting-line solver developed by IFPEN [30], and SOWFA is a library based on the CFD solver OpenFOAM developed at the National Renewable Energy Laboratory [31].

A slight over-estimation of the loads calculated by Meso-NH + ALM can be observed around $r = 1.5m$ in the 15 m/s case. Conversely, the computed loads show an under-evaluation at the tip of the blade for the 15m/s and 24m/s cases. It might be due to the improper use of the tip-loss correction. In fact, without the tip loss correction, the CASTOR results is matched at 24m/s. Nevertheless, the results seem in good agreements with both the experimental and the

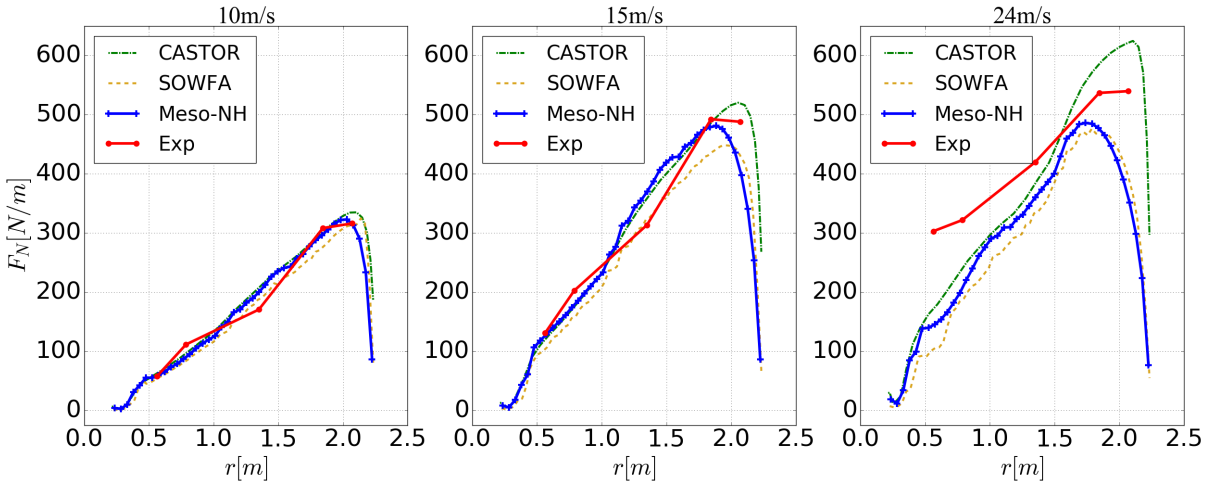

Figure 2. Comparison of normal F_N forces per unit of length along the blades for the three cases (10m/s, 15m/s and 24m/s), with the experiment, CASTOR and SOWFA simulations. Details about these simulations can be found in [30].

numerical data. Besides, it can be already mentioned that, in the next study concerning the Horns Rev 1 photo case, the operating state of the wind turbine is in a turbulent wake state close to the $10m/s$ case, where the Tip Speed Ration is high ($TSR \simeq 10$). Thus, the coupled tool between Meso-NH and the Actuator Line Method will be used to explore wind farm wakes such as the Horns Rev 1 Photo Case.

4. Wind farm wake

4.1. The Horns Rev 1 Photo case

The Horns Rev 1 wind farm is located at the east of the North Sea, about 10 km from the Danish coast. It was the first large scale offshore wind farm in the world, hence its worldwide interest. The farm has a total of 80 Vestas V80-2.0 MW units, arranged in a regular layout as a rhomboid shape of 5 km x 3.8 km (8 horizontal and 10 vertical rows) with a minimal distance of 7 diameters between the closest wind turbines.

In the morning of February 12, 2008 the photographer Christian Steiness took two photos from a helicopter of the wind park (Figure 4 and 6). They showed a physical evidence of the interaction of a wind farm with the lowest layers of the atmosphere. This well known photo, taken at 10:10 UTC, shows the formation of clouds downwards the Horns Rev 1 wind farm because of its presence. A description of the meteorological conditions and the process that would have led to the formation of these clouds can be found in [2]. At this moment, a layer of cold humid air above a warmer sea surface re-condensates to fog in the wake of the turbines. The triggering of the re-condensation is due to the wind turbines motion. The operating rotors caused, some distance downwind the wind turbines, upward movements of humid and warm air from near the sea surface, and, at the same time, downward movements of dry, adiabatically cooled air from the top of the rotor. The rotational pattern of spiraling bands produces the large scale structure of the wake fog.

4.2. Numerical Set-Up

Meteorological conditions The scarcity of meteorological information available to recreate the atmospheric state is one of the main difficulties to simulate the Horns Rev 1 Photo Case phenomenon. Hasager *et al.* [2] already collected an important amount of observational data

from a large range of sources. The on-site meteorological mast provided measurements of temperature at 16m and 64m and the sea temperature. It also provided measurements of wind velocity at three different heights (30m, 40m and 70m) and wind direction at 28m and 68m. In order to have a better description of the vertical structure of the atmosphere, this work also uses reanalysis data from the Modern-Era Retrospective analysis for Research and Applications (MERRA).

The simulation of this photo case is performed in two stages. First, a precursor simulation is performed. The 3D state of the atmosphere without the wind farm is set-up. Then, the wind turbines are incorporated and the previous simulation is used as initial condition. Figure 3 presents the different vertical profiles of the precursor simulation. The dashed blue lines correspond to the profiles used as input to initialize the whole domain, based on met mast and reanalysis data. The solid ones correspond to the horizontally averaged vertical profiles obtained after three hours of simulation.

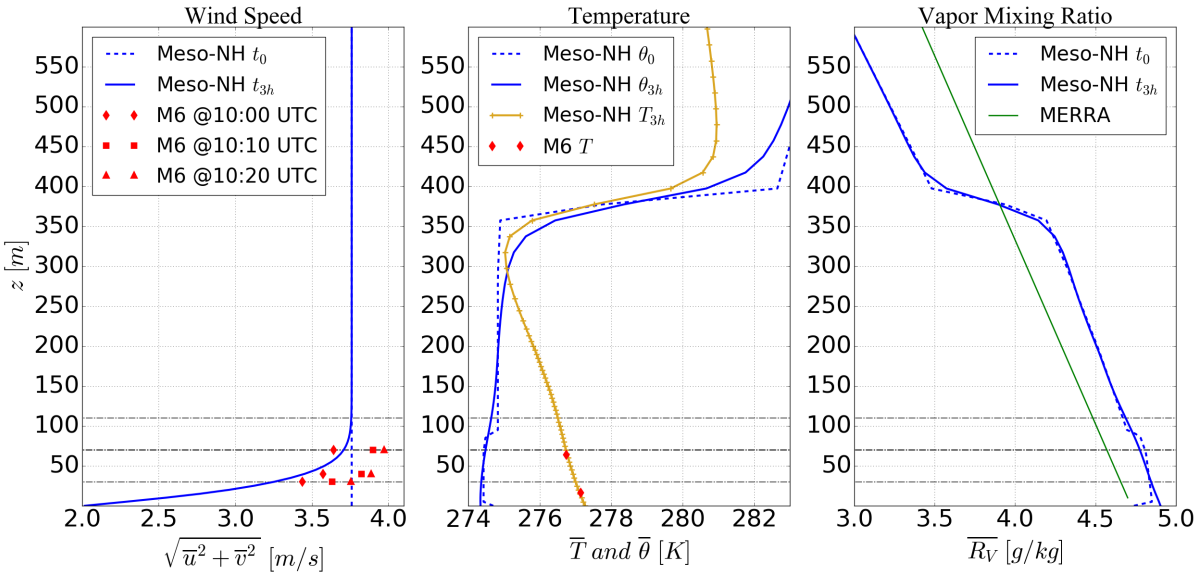

Figure 3. Wind speed, temperature and vapor mixing ration profiles. M6 Data from [2].

As initial conditions, a constant value along the vertical is used for the wind velocity. This value corresponds to the geostrophic wind forcing the field. Its intensity and direction have been adjust to reach the measured wind velocity profile measured by the met mast M6 after three hours of simulation, by taking into account the friction from the ground and the Ekman Spiral due to the Coriolis effects. The logarithmic shape of the temporally and horizontally averaged wind velocity profile is reached and fits well with the measurements, as show in Figure 3. Thanks to the reanalysis data, a $400m$ height atmospheric boundary layer has been determined, and a strong temperature inversion for the potential temperature θ has been set at this height. Besides, several clues indicate the presence of a surface layer inside the boundary layer: in order to maintain the sea smoke under the rotor level and because it is the beginning of the day, a second and weaker inversion must be present. This is why a surface layer has been introduced at $90m$ with an inversion about $\Delta\theta = -0.4K$. This value has been chosen after a sensitivity study, showing that no clouds would appear with a higher one: the air masses becomes too warm in the upper part of the rotor to condensate. Both initial conditions, in the surface layer and in the residual layer, are neutral. As show in Figure 3, these conditions become slightly stable after three hours of simulation, but the surface layer and the residual layer

are still distinguishable. It can also be observed that the temperature T is in good agreement with the met mast data. The measured sea temperature was about $277.85K$ at $-3m$ depth with a precision about $\pm 0.7K$. After a sensitivity analysis, the sea temperature has been set to $277.35K$. A warmer sea would generate too much turbulence, involving unstable conditions and a cloud formation with a different aspect from the layered sea smoke that can be observed in the photo. The pressure at the ground is about $103890Pa$. There is no proper measurement for the vapor mixing ratio R_V. Since the pressure and the temperature are given by measurements, this variable has to be found, respecting the order of magnitude given by the MERRA reanalysis. Compared to the reanalysis, higher values have been set near the ground. The surface layer allows to maintain the vapor in this layer after the 3 hours simulation.

For this simulation, the domain size is about $L_x = 600m \times L_y = 10000m \times L_z = 837.5m$, with a $5m$ horizontal resolution and a time step about $\Delta t = 1s$. The vertical resolution is about $5m$ below $200m$, and is stretched by 20% above until it reached $20m$ of resolution. The lateral boundary conditions are cyclic. The sea surface is modeled using the Sea Flux Scheme [32]. In order to treat micro-physics phenomena, the single-moment 6-class scheme ICE3 is used [33]. The long-wave radiation is computed following [34], and the shortwave following [35].

Idealized wind farm In the second stage, the wind turbines are introduced. For this simulation, only one row of eight wind turbines is modeled. The layout, shown in Table 2, is based on [36]. Thanks to the lateral cyclic conditions and the domain dimensions, this row of wind turbines can be seen as a row inside an entire wind farm. This idealized wind park, close to the Horns Rev 1 farm, does not respect the rhomboid shape. It can also be noted that if the distance between two rotors in a same row is respected, it is not the case for the distance between the rows: this distance is equal to the domain width (because of the cyclic conditions), which is about 600m instead of 556m. In fact, to solve the Poisson's equation, the pressure solver of Meso-NH uses a fast Fourier transform which imposes a finite number of possibilities for the domain size: the number of cells in each direction has to be a multiple of 5, 3 and 2.

Table 2. Idealized wind farm layout description with angular velocities.

Wind Turbine	X (m)	Y (m)	Ω (RPM)	Wind Turbine	X (m)	Y (m)	Ω (RPM)
n°1	300	500	13.16	n°5	300	2740	9.76
n°2	300	1060	10.03	n°6	300	3300	11.25
n°3	300	1620	11.94	n°7	300	3860	11.49
n°4	300	2180	10.13	n°8	300	4420	11.56

The wind direction is about 180° and the yaw angle of the wind turbines is set to zero. According to the SCADA data from [2], turbines operated near the cut-in speed. For the simulated row, the angular velocity imposed to the i^{th} rotor is the averaged angular velocity of the rotating wind turbines in the horizontal row number i (Table 2). The Vestas V80 is a 80m diameter three bladed rotor with a hub placed at 70m. The twisted and tapered blades are based on FFA-W3-301, FFA-W3-241, FFA-W3-221, NACA-63-221 and NACA-63-218 airfoils from root to tip, according to [36]. The pitch angle is set to 0° because of the near cut-in operation. For the Actuator Line Method, the blades are divided into 42 element points, and the tip loss correction of Glauert is used. The time step is set to $0.05sec$.

4.3. Results

A vertical cross-section in the mid-plane of the relative humidity R_h computed after twenty minutes of simulation can be seen in Figure 5. The effect of the wind farm in this field is observable, and shows very similar patterns to the photo (Figure 4). In fact, around the wind farm, an important value of the relative humidity can denote the presence of the sea smoke. In the near wake of the first wind turbine, the constant stretched cloud above the hub height is recognizable, and seems to be directly took off from the lower level by the blades.

Figure 4. Photograph of the Horns Rev 1 wind farm (12/02/2008 around 10:10 UTC) from southeast. Courtesy Vattenfall. Photographer: Christian Steiness

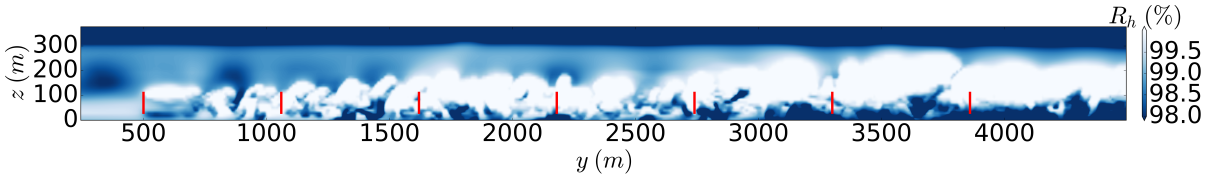

Figure 5. Mid-plane vertical cross-section of the relative humidity. The red plain lines (–) indicate the locations of wind turbines.

Figure 7 shows a 3D plot of cloud mixing ratio iso-contour. As it can be noticed, the sea smoke near the ground is not shown with this variable: even if the relative humidity is high (around 100%), the water vapor does not condensate. The main feature in this figure is the well represented helical pattern of the wake in an increasing conical shape, showing the ability of this new coupled tool to reproduce the Horns Rev 1 photo case phenomena in order to analyze them. At this very moment, the inversion layer reached the hub height. Thus, the operating wind turbines mixed two different air mass from the surface layer and the residual layer with their rotational movement, involving the particular phenomenon.

5. Discussion and Conclusion

A deeper knowledge about the interaction of wind turbines with the lowest levels of the atmosphere is necessary. In this sense, a new tool was developed to explore these interactions. The new numerical tool is a coupled model between the Actuator Line Method and the non-hydrostatic mesoscale atmospheric model Meso-NH based on the Large Eddy Simulation framework. In the aim of performing a validation of the Meso-NH + ALM model, comparisons against New MEXICO measurements have been performed, showing that the predicted loads

Figure 6. Photograph of the Horns Rev 1 wind farm (12/02/2008 around 10:10 UTC) from south. Courtesy Vattenfall. Photographer: Christian Steiness.

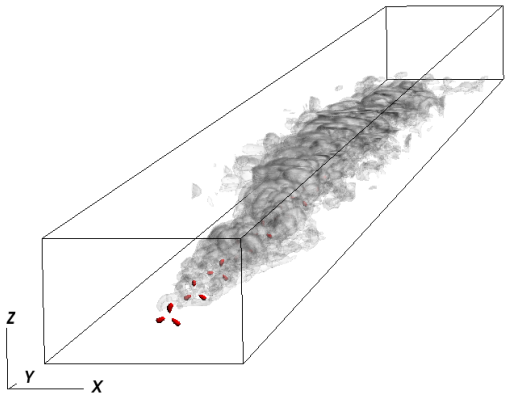

Figure 7. 3D plot of cloud mixing ratio iso-contour (greys). Wind turbine blades are represented in red.

are well evaluated for high tip speed ratio operation state. A better load distribution should be developed to improve the results at lower TSR.

Once the new tool was validated, it was used to simulate an idealized case of the Horns Rev 1 Photo case. To reproduce the meteorological conditions that gave rise to this phenomenon, a spin-up simulation was carried out based on in situ met-mast measurements and MERRA reanalysis data. The obtained 3D atmospheric state showing good correlation with the measurements was used, as initial conditions, in the idealized simulation where the reduced wind farm was introduced. The main and conclusive result of this simulation was the well developed cloud pattern that is evidenced when plotting both the relative humidity and the resulting cloudiness. Actually, the liquid water is slightly under-estimated by the model. It can be due to the aerosol consideration: further study will be carried out about the micro-physical scheme used. However, the particular spiral pattern is very similar to the photo and shows the capability of this new tool to simulate dynamically the wakes and represent their impact and interaction with the atmospheric variables.

It should also be mentioned that this phenomenon can only appear in really particular meteorological conditions. In fact, the sensitivity studies carried out showed that little changes in temperatures would led to a global fog formation or nothing at all. In other words, this case occurs within a critical equilibrium between two possible meteorological conditions.

Future work will pursue the study of the Horns Rev 1 Photo Case, simulating the whole farm at a finer resolution, with the aim of improving the analysis of the phenomena. The space and time span of the impact will be evaluated, and other parameters such as the potential temperature will be investigated. Furthermore, not only because offshore wind turbines will become larger but also because the atmospheric boundary layer is generally lower over the sea, more theoretical studies will be conducted in order to forecast the potential interactions that could occur when rotors are operating in the capping inversion layer.

5.1. Acknowledgments

New MEXICO data used have been supplied by the consortium which carried out the EU FP5 project MEXICO: “Model rotor EXperiments In COntrolled conditions”. The authors wish to thank the IEA Wind Task 31 WakeBench which provided the description of the Horns Rev 1 wind farm and of the Vestas80 wind turbine model.

References

[1] Barthelmie R J et al. 2009 Wind Energy: An International Journal for Progress and Applications in Wind Power Conversion Technology **12** 431–444
[2] Hasager C B, Rasmussen L, Peña A, Jensen L E and Réthoré P E 2013 Energies **6** 696–716
[3] Boorsma K and Schepers J 2014 New MEXICO experiment: Preliminary overview with initial validation (ECN)
[4] Lac C et al. 2018 Geoscientific Model Development **11** 1929–1969
[5] Lafore J P et al. 1998 Annales Geophysicae **16** 90–109 URL `https://www.ann-geophys.net/16/90/1998/`
[6] Sommeria G 1976 Journal of the Atmospheric Sciences **33** 216–241
[7] Redelsperger J L and Sommeria G 1981 Boundary-Layer Meteorology **21** 509–530
[8] Redelsperger J L and Sommeria G 1986 Journal of the atmospheric sciences **43** 2619–2635
[9] Cuxart J, Bougeault P and Redelsperger J L 2000 Quarterly Journal of the Royal Meteorological Society **126** 1–30
[10] Deardorff J W 1980 Boundary-Layer Meteorology **18** 495–527
[11] Durran D R 1989 Journal of the atmospheric sciences **46** 1453–1461
[12] Mesinger F, Arakawa A and Sundqvist H 1976 Numerical methods used in atmospheric models vol 1 (World Meteorological Organization, International Council of Scientific Unions)
[13] Jabouille P et al. 1999 Parallelization of the french meteorological mesoscale model mésonh European Conference on Parallel Processing (Springer) pp 1417–1422
[14] Sorensen J N and Shen W Z 2002 Journal of fluids engineering **124** 393–399
[15] Rankine W 1865 Trans. Inst. Naval Architects **6** 13–39
[16] Froude R E 1889 Trans. Inst. Naval Architects **30** 390
[17] Mikkelsen R 2003 Actuator disc methods applied to wind turbines Ph.D. thesis Technical University of Denmark
[18] Ivanell S, Sørensen J N and Henningson D 2007 Numerical computations of wind turbine wakes Wind Energy (Springer) pp 259–263
[19] Ivanell S, Sørensen J N, Mikkelsen R and Henningson D 2007 Numerical analysis of the tip and root vortex position in the wake of a wind turbine Journal of Physics: Conference Series vol 75 (IOP Publishing) p 012035
[20] Troldborg N, Sørensen J N and Mikkelsen R F 2009
[21] Porté-Agel F, Wu Y T, Lu H and Conzemius R J 2011 Journal of Wind Engineering and Industrial Aerodynamics **99** 154–168
[22] Churchfield M, Lee S, Moriarty P, Martinez L, Leonardi S, Vijayakumar G and Brasseur J 2012 A large-eddy simulation of wind-plant aerodynamics 50th AIAA Aerospace Sciences Meeting including the New Horizons Forum and Aerospace Exposition p 537
[23] Martinez L, Leonardi S, Churchfield M and Moriarty P 2012 A comparison of actuator disk and actuator line wind turbine models and best practices for their use 50th AIAA Aerospace Sciences Meeting including the New Horizons Forum and Aerospace Exposition p 900
[24] Nathan J 2018 Application of actuator surface concept in LES simulations of the near wake of wind turbines Ph.D. thesis École de technologie supérieure
[25] Jha P K, Churchfield M J, Moriarty P J and Schmitz S 2014 Journal of Solar Energy Engineering **136** 031003
[26] Martínez-Tossas L A, Churchfield M J and Meneveau C 2016 A highly resolved large-eddy simulation of a wind turbine using an actuator line model with optimal body force projection Journal of Physics: Conference Series vol 753 (IOP Publishing) p 082014
[27] Nathan J, Masson C and Dufresne L 2018 Wind Energy Science **3** 905–917
[28] Glauert H 1935 Airplane propellers Aerodynamic theory (Springer) pp 169–360
[29] Churchfield M J, Schreck S J, Martinez L A, Meneveau C and Spalart P R 2017 An advanced actuator line method for wind energy applications and beyond 35th Wind Energy Symposium p 1998
[30] Blondel F, Ferrer G, Teixeira D and Cathelain M 2017 S19-Mécanique pour l'énergie éolienne
[31] Churchfield M, Lee S and Moriarty P 2012 Overview of the simulator for wind farm application (sowfa)
[32] Belamari S 2005 Marine EnviRonment and Security for the European Area–Integrated Project (MERSEA IP), Deliverable D **4**
[33] Pinty J P and Jabouille P 1998 6b. a mixed-phased cloud parameterization for use in a mesoscale non-hydrostatic model: simulations of a squall line and of orographic precipitation Conference on Cloud Physics: 14th Conference on Planned and Inadvertent Weather Modification pp 17–21
[34] Mlawer E J, Taubman S J, Brown P D, Iacono M J and Clough S A 1997 Journal of Geophysical Research: Atmospheres **102** 16663–16682
[35] Fouquart Y and Bonnel B 1980 Beitraege zur Physik der Atmosphaere **53** 35–62
[36] Hansen K 2012 IEA WInd Task 31 Wakebench